3-Dimensional Trajectory Optimization for UAV-Based Post-Disaster Data Collection

Renkai Zhao and Gia Khanh Tran *

Posted Date: 8 April 2025

doi: 10.20944/preprints202504.0609.v1

Keywords: UAV; data collection; Trajectory Optimizaion; location set cover problem; k-means clustering; genetic algorithm

 doi:10.20944/preprints202504.0609.v1

Article

3-Dimensional Trajectory Optimization for UAV-Based Post-Disaster Data Collection

Renkai Zhao [1] and Gia Khanh Tran [2,*]

Department of Electrical and Electronic Engineering, School of Engineering, Institute of Science Tokyo
* Correspondence: khanhtg@mobile.ee.titech.ac.jp

Abstract: In Japan, natural disasters occur frequently. Serious disasters may cause damage to traffic networks and telecommunication infrastructures, leading to the occurrence of isolated disaster areas. In this article, unmanned aerial vehicles (UAV) are used for data collection instead of unavailable ground base stations in isolated disaster areas. Detailed information about the damage situation will be collected from the user equipments (UE) by a UAV through a fly-hover-fly procedure, and then will be sent to the disaster response headquarters for disaster relief. However, mission completion time minimization becomes a crucial task, considering the requirement of rapid response and the battery constraint of UAVs. Therefore, the author proposed a 3-dimentional UAV flight trajectory, discussing the optimal flight altitude and placement of hovering points by transforming the problem to a location set cover problem (LSCP). The simulation results have shown the feasibility of the proposed method to reduce the mission completion time.

Keywords: UAV; data collection; Trajectory Optimizaion; location set cover problem; k-means clustering; genetic algorithm

1. Introduction

In Japan, natural disasters such as earthquakes, tsunamis and typhoons occur frequently. These disasters may cause significant damage to communication infrastructure such as base stations and cables. In 2011, approximately 29,000 base stations were reported being shut down after the Great East Japan Earthquake [1]. In addition, damages to the access to the outside world result in the occurrence of isolated disaster areas [2]. Due to the cutoff of the national highway, Yamamoto, Miyagi was completely isolated until 4 days after the disaster [3].

Because of the difficulty in obtaining disaster information from the isolated disaster areas, the early deployment of rescue events is hindered. Therefore, it is necessary to introduce communication systems which do not rely on existing communication infrastructures on the ground.

Non-terrestrial networks (NTN), which include platforms operating between 0.1 to 2000 km altitudes such as unmanned aerial vehicles (UAV), high altitude platforms (HAPs), low earth orbit satellites (LEO) etc., are nowadays popular as post-disaster communication solutions. For non-real-time temporary data collection mission in isolated disaster areas, the use of UAVs, which are also commonly known as drones, is considered suitable because of their low cost, high mobility and high flexibility.

2. Related Works

UAV-based data collection has been discussed in several previous studies as summarized in Table 1. In [4], the article dealt with the issue of improving rural connectivity. Path planning and UAV relays were conducted to improve quality in rural area. Unfortunately, the paper only focused on the connectivity. In [5], the authors considered an obstacle-aware deployment of UAV, where path optimization in obstacle-heavy environments was conducted. UAV in this paper was employed as a relay rather than a data collector as considered in this paper. In [6], the authors proposed a disaster

 doi:10.20944/preprints202504.0609.v1

monitoring system via multi-UAV coordination. The paper only focused on UAV coordination but did not consider how to optimize data collection. In [7], UAV-based surveillance system was introduced where multi-UAV collaboration was done via Deep Reinforcement Learning (DRL). Since this system was specific to surveillance, it is not generally applicable for the scenario of data collection considered in this paper.

Table 1. Related Works

Study	Application Focus	Key Technologies	Contributions	Limitations
[4]	Rural connectivity enhancement	Path planning and UAV relays	Focused on improving link quality in rural zones	Limited to rural; not scalable for high-mobility urban networks
[5]	Obstacle-aware deployment	Area barrier-aware deployment	Path optimization in obstacle-heavy environments	Focuses on fixed deployment scenarios
[6]	Disaster monitoring	Multi-UAV coordination	Disaster-focused UAV coordination and communication	Does not focus on data collection optimization
[7]	Surveillance via DRL	Deep Reinforcement Learning (DRL)	Multi-UAV collaboration using DRL	Specific to surveillance, not general data collection
[8]	Data collection	Multi-armed bandit (MAB)	Consideration of energy consumption of UAV and UE	2D trajectory optimization
[9]	Data collection	Markov decision making process (CMDP)	Consideration of energy consumption of UE	No consideration of energy consumption of UAV
[10]	Data collection	Travelling Salesman Problem (TSP)	Completion time minimization	2D trajectory optimization
[11]	Data collection	Segment-based trajectory optimization algorithm (STOA)	Joint optimization of trajectory and link scheduling	2D trajectory optimization
[12]	Data collection	Single LAP covering a whole area	Coverage enhancement	Limited data rate
[13]	IoT networks	K-means clustering	Energy harvesting efficiency	No discussion on data transmission
[14]	Flying base station	Offline-based online adaptive (OBOA) design	Wind consideration	No discussion on completion time
[15]	Flying base station	3D placement	Maximum coverage of UEs with different QoS requirements	No discussion on completion time

There were also works that focused on the use of UAVs for data collection. The author of [8] optimized the 2-dimensional trajectory with multi-armed bandit (MAB) algorithm, considering the energy consumption of the UAV and the UEs, to maximize the throughput. In [9], the throughput maximization problem is transformed to a constrained Markov decision-making process (CMDP), considering the energy consumption of the UEs. In addition, the author of [10] aimed to minimize

 doi:10.20944/preprints202504.0609.v1

the mission completion time by optimizing the transmission power of UEs and the flight trajectory. In [11], flight altitude, trajectory, velocity and link scheduling are considered for completion time minimization. Unfortunately, all these works were restricted to the 2D optimization of trajectory as compared to the 3D trajectory optimization in this paper. The relation between the flight altitude and the coverage is shown in [12] that higher altitude brings larger coverage via a high-altitude platform (LAP) rather than a UAV. In [13], 3-dimensional locations of the UAV are decided with k-means clustering, without the discussion on data transmission. In [14], a 3-dimensional trajectory is optimized to maximize the energy efficiency, considering the presence of wind. The author of [15] proposed a maximal weighted area (MWA) algorithm to solve the 3-dimensional placement problem of UAV base stations. Unfortunately, these works did not discuss on the completion time or the time restriction of collecting data.

Different from the above-mentioned conventional works, in this article, we focus on the 3D optimization of the flight altitude of the UAV, examining the completion time reduction effect by adopting the 3-dimensional trajectory and a scheduling mechanism to minimize the time required for the data collection process.

3. System Architecture

As shown in Figure 1, the simulation scenario in this article is that a single UAV collects data from user equipments (UE) such as smartphones and tablets owned by users in the isolated disaster area.

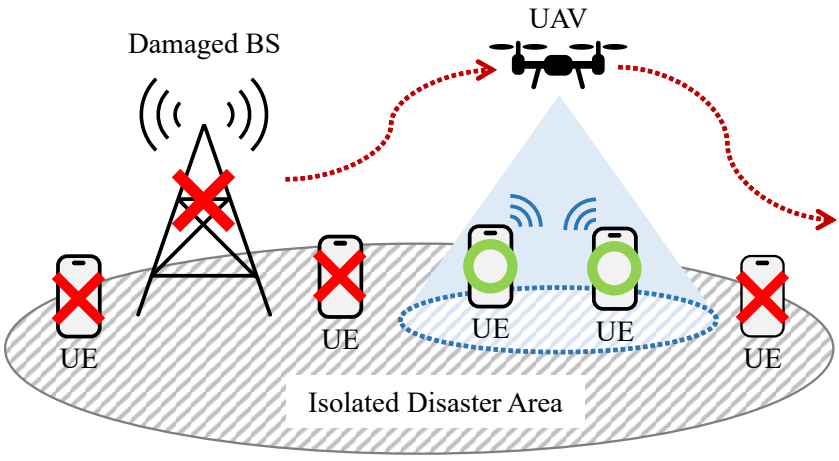

Figure 1. Overview of the System

The UAV is assumed to collect data from the UEs when hovering, and there is no data transmission between the UAV and the UEs during flight. As shown in Figure 2, the 3-dimensional trajectory proposed by this article optimizes the UAV's flight altitude. In areas with dense UE distribution, the UAV's flight altitude is increased to achieve a larger coverage area. In contrast, in areas with scattered UE distribution, the UAV's flight altitude is reduced to achieve higher throughput.

The detailed process of the data collection mission is shown as below:

1. Collect location information of UEs by other systems such as HAPS, LEO etc.;
2. The UAV departures from the starting point;
3. The UAV flies to the next hovering point;
4. The UAV collects data from all covered UEs;
5. Repeat 3~4 until all UEs' data is collected;
6. The UAV return to the starting point;
7. Send the collected data to the disaster response headquarter.

Note that for simplicity, 1 and 7 are not covered in this article.

 doi:10.20944/preprints202504.0609.v1

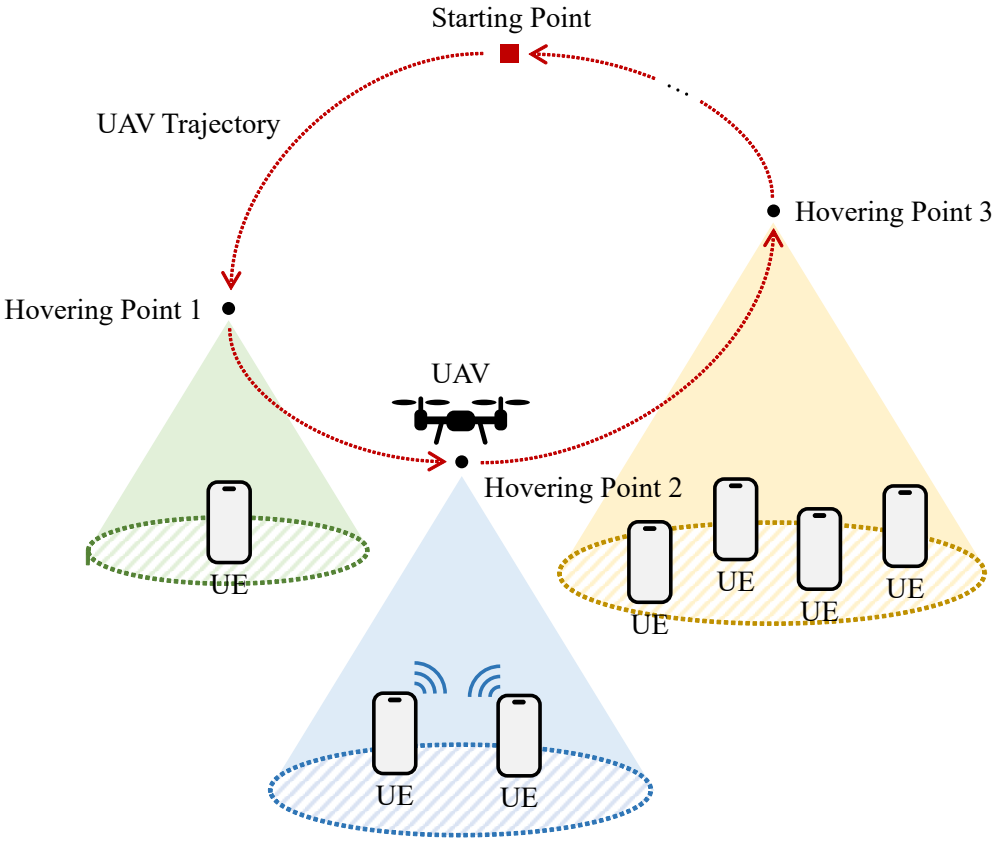

Figure 2. Process of the UAV-Based Data Collection Mission

For simulation, a 500×500m flat urban area is assumed as the simulation environment. As the sample shown in Figure 3, M UEs are randomly distributed in this area. The starting point of the UAV is set in the center of the area as $(250, 250, 0)$, and the location of the UAV at time t is assumed as $(X_t^{\mathrm{UAV}}, Y_t^{\mathrm{UAV}}, H_t^{\mathrm{UAV}})$, the location of the m $(m \leq M)$-UE is assumed as $(X^{m-\mathrm{UE}}, Y^{m-\mathrm{UE}}, H^{m-\mathrm{UE}})$. Note that for simplicity, the UEs are assumed not to change their location.

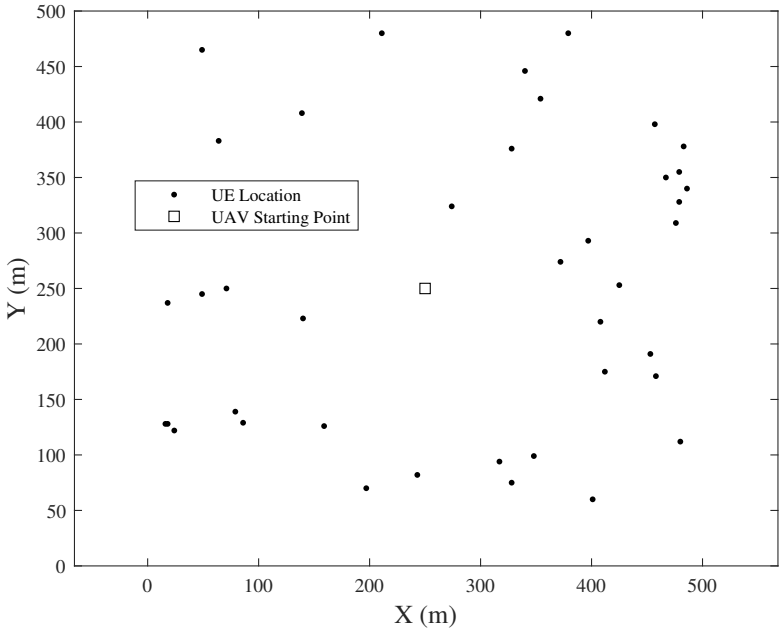

Figure 3. Sample of UE Distribution ($M = 40$)

 doi:10.20944/preprints202504.0609.v1

We adopt the 2.4 GHz band for data transmission, because it can be easily integrated with the hardware of UEs nowadays. For simplicity, the shape of the buildings is ignored. Thus, the data transmission model between the UAV and the UEs is defined with the possibilities of Line-of-Sight (LoS) and Non-Line-of-Sight (NLoS) propagation. As shown in Figure 4, LoS propagation occurs only when there is no obstacle between the UAV and the UE.

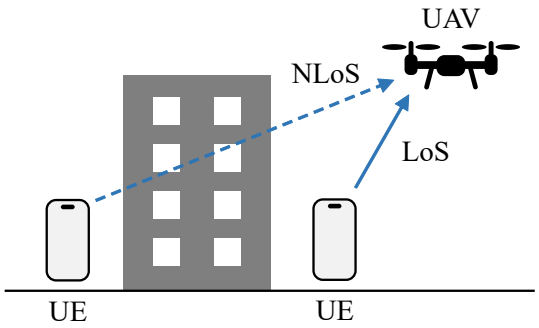

Figure 4. LoS and NLoS Propagation

The LoS and NLoS propagation loss between the UAV and the m-UE at time t $L_{m,t}^{\text{LoS}}$, $L_{m,t}^{\text{NLoS}}$ are given below:

$$L_{m,t}^{\text{LoS}} = 20\log_{10}(\frac{4\pi f_c}{c} d_{m,t}) + \eta_{\text{LoS}} \tag{1}$$

$$L_{m,t}^{\text{NLoS}} = 20\log_{10}(\frac{4\pi f_c}{c} d_{m,t}) + \eta_{\text{NLoS}} \tag{2}$$

where $20\log_{10}(\frac{4\pi f_c}{c} d_{m,t})$ is the free space propagation loss (FSPL), η_{LoS}, η_{NLoS} are respectively the LoS and NLoS excessive loss, $d_{m,t}$ is the Euclidean distance between the UAV and the m-UE at time t.

According to [12], the possibilities of LoS and NLoS propagation $P_{m,t}^{\text{LoS}}$, $P_{m,t}^{\text{NLoS}}$ are given below:

$$P_{m,t}^{\text{LoS}} = \frac{1}{1 + a\exp(-b(\theta_{m,t} - a))} \tag{3}$$

$$P_{m,t}^{\text{NLoS}} = 1 - P_{m,t}^{\text{LoS}} \tag{4}$$

where a, b are environment S-curve parameters, $\theta_{m,t}$ is the elevation angle from the m-UE to the UAV.

Thus, the propagation loss between the UAV and the m-UE at time t $L_{m,t}$ can be calculated by:

$$L_{m,t} = P_{m,t}^{\text{LoS}} L_{m,t}^{\text{LoS}} + P_{m,t}^{\text{NLoS}} L_{m,t}^{\text{NLoS}} \tag{5}$$

From the Shannon–Hartley Theorem [16], the maximum data rate between the UAV and the m-UE at time t $C_{m,t}$ can be calculated by:

$$C_{m,t} = \alpha_{m,t} B \log_2 (1 + \frac{P_{\text{tx}}}{\sigma L_{m,t}}) \tag{6}$$

where $\frac{P_{\text{tx}}}{\sigma L_{m,t}}$ is the signal noise ratio (SNR) between the UAV and m-UE, the $\alpha_{m,t}$ is an indicator decided by the connection status between the UAV and m-UE, which is defined as below:

$$\alpha_{m,t} = \begin{cases} 1 & (\text{if } m\text{-UE at transmission mode}) \\ 0 & (\text{if } m\text{-UE at idle mode}) \end{cases} \tag{7}$$

 doi:10.20944/preprints202504.0609.v1

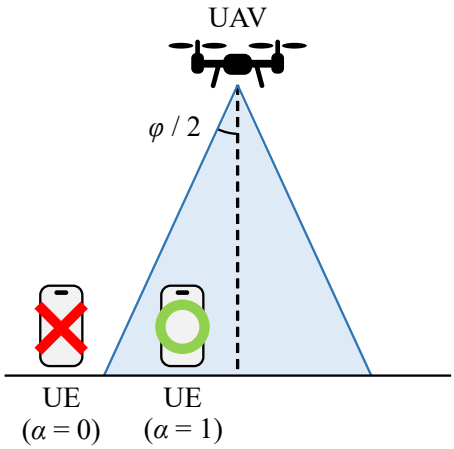

Figure 5. Connection Status between the UAV and the UE.

In addition, the simulation parameters used in this article are shown in Table 2.

Table 2. Simulation Parameters

Parameter	Value
Frequency f_c (MHZ)	2412
Bandwidth B (MHz)	22
Boltzmann Constant k_B	1.38×10^{-23}
Tempreture T (K)	298
Enviroment S-Curve Parameter a	9.61
Enviroment S-Curve Parameter b	0.16
LoS Additional Loss η_{LoS}	1
NLoS Additional Loss η_{NLoS}	20
UAV Antenna Type	Directional
UAV Antenna Half Width (rad)	$\pi/4$
UAV Forward Velocity v^{forward} (m/s)	14
UAV Ascent Velocity v^{ascent} (m/s)	5
UAV Descent Velocity v^{descent} (m/s)	4
UE Antenna Type	Omnidirectional
UE Transmission Power P_{tx} (mW)	200
UE Maximum Data Size Φ_{max} (MB)	10

4. Methods

The 3-dimensional trajectory optimization is divided into 2 parts: hovering points placement and trajectory decision. The locations of the hovering points are decided by the distribution of the UEs. After the hovering points are decided, the trajectory which passes through all hovering points with the minimum time is needed to be decided, which can be considered as a classic traveling salesman problem (TSP).

4.1. K-Means Clustering for Placement of Hovering Points

The k-means clustering is known as a non-hierarchical cluster analysis method, classifying multiple elements into k clusters. K-means has been adopted by related studies to UAV communication networks, such as [17], where it is used to solve the placement problem of multiple UAV base stations. In this article, k-means is considered feasible to solve the placement problem of the UAV hovering points.

Now apply k-means to the UE distribution shown in Figure 3, the UE clustering by k-means with varying number of clusters k is shown in Figure 6. The dotted circles represent the required coverage area to cover all UEs belonging to each cluster, while the locations of the hovering points are assumed as the center points of the clusters. However, it is suggested from [17] that the center points of the

 doi:10.20944/preprints202504.0609.v1

clusters are not the optimal locations for the hovering points. As the results shown in Figure 6, there are empty areas with no UE covered in the coverage areas. To enhance the transmission efficiency, a geometric method, the minimum inclusion circle, was introduced by [17], while it only works when the UEs are all on the same plane.

In this article, we proposed to search for the optimal location of hovering points through numerical computation. Hill climbing algorithm (HC), a simple local search method, is adopted. Minimum SNRs between the UAV and the UEs from each candidate point are calculated. And then the location of the hovering points will be updated to the new location with the largest minimum SNR, until the minimum SNR does not change any more.

However, the k-means clustering has 2 critical problems:

- For realistic problems, the number of clusters k is often difficult to be determined in advance.
- Conditions such as the limitation of UAV's flight altitude, which is 150 m according to the law in Japan, is hard to be included. As the results shown in Figure 6, the flight altitude is too high when k is small.

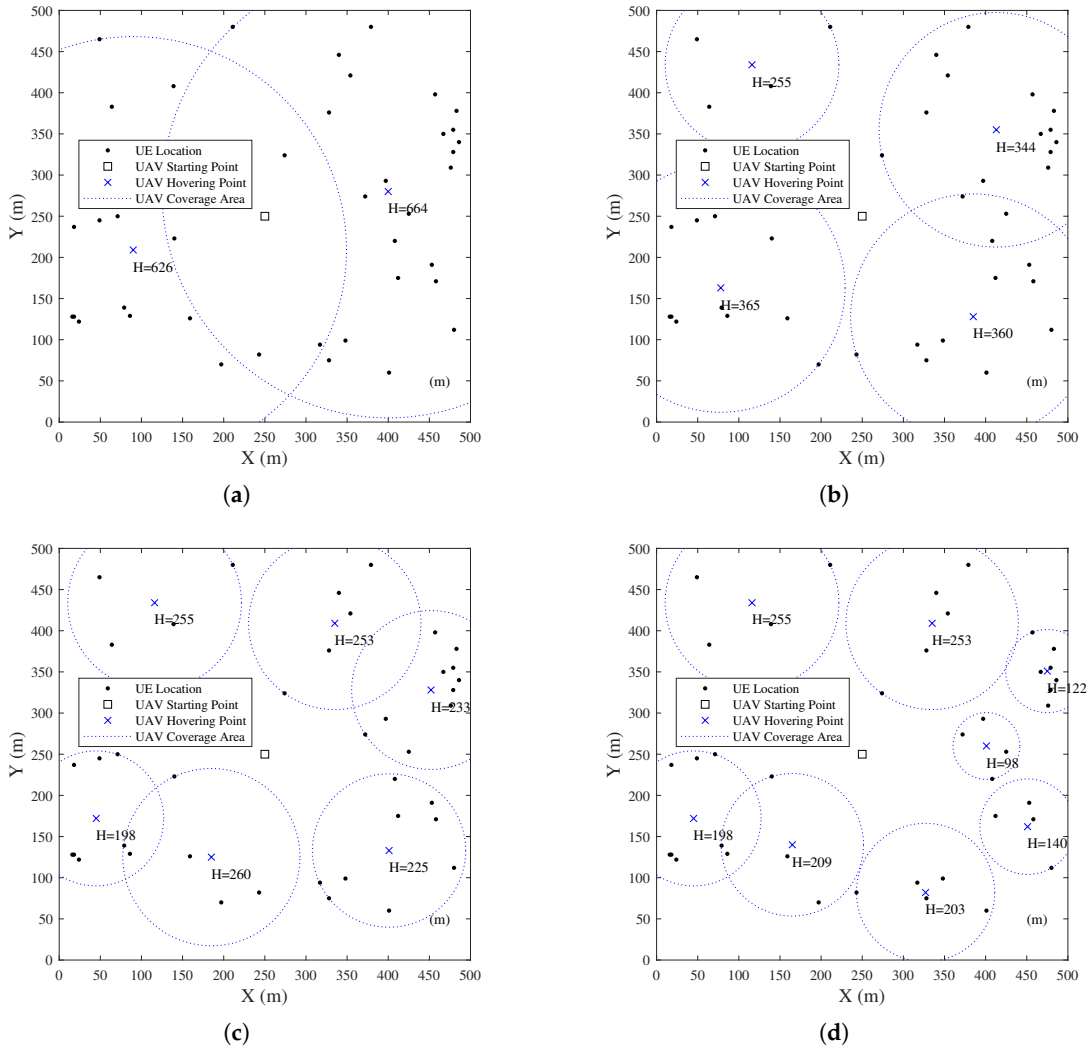

Figure 6. *Cont.*

Preprints.org (www.preprints.org) | NOT PEER-REVIEWED | Posted: 8 April 2025 doi:10.20944/preprints202504.0609.v1

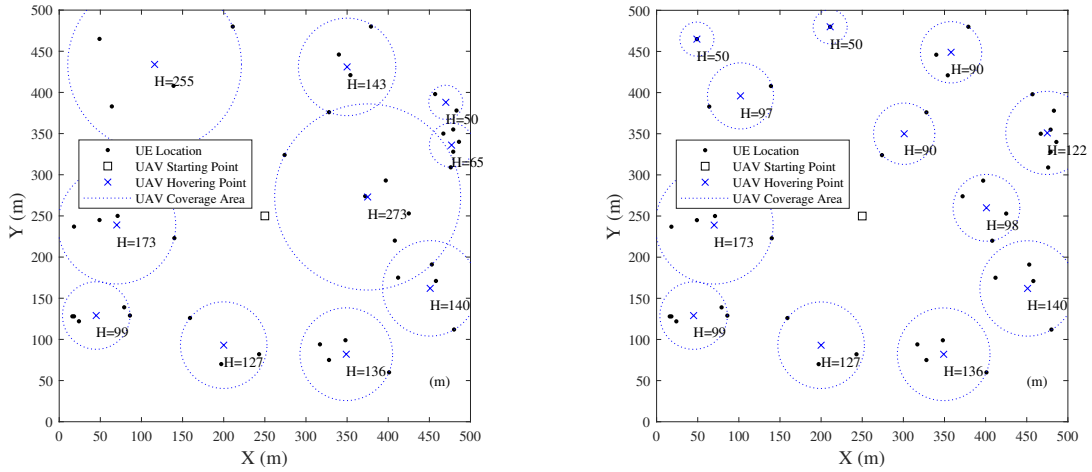

(**e**) (**f**)

Figure 6. UE Clustering by K-Means: (**a**) $k = 2$ (**b**) $k = 4$ (**c**) $k = 6$ (**d**) $k = 8$ (**e**) $k = 10$ (**f**) $k = 12$.

Therefore, we proposed a sequential k-means clustering method to search for the minimum k. If the result of the UE clustering satisfies the condition of the UAV's flight altitude, the present k will be adopted. Otherwise, the operation will continue by increasing k.

4.2. Genetic Algorithm for Placement of Hovering Points

To fundamentally solve the problems of traditional clustering methods, we transform the hovering points placement problem to a location set covering problem (LSCP) [18], which is commonly used to solve the placement problems of public facilities. The definition of LSCP is given as follows:

$$\min . \quad \sum_{j \in J} x_j \tag{8}$$

$$\text{s.t.} \quad 1 \leq \sum_{j \in J} a_{ij} x_j \qquad \forall i \in I \tag{9}$$

$$x_j \in \{0, 1\} \qquad \forall j \in J \tag{10}$$

$$a_{ij} = \begin{cases} 1 & \text{(if distance between } i \text{ and } j \leq \text{coverage radius)} \\ 0 & \text{(if distance between } i \text{ and } j > \text{coverage radius)} \end{cases} \tag{11}$$

According to the definition of LSCP, the problem can be described as searching for the minimum number of hovering points that enable covering all UEs in a certain area. The coverage radius of the facility is defined as the maximum coverage radius of the UAV, which is 62.132 m, based on the limitation of UAV's flight altitude in this article.

The basic strategy to solve the LSCP in this article is the greedy algorithm, which continues to select the location of the hovering point that can cover the largest number of UEs until all UEs have been covered. Although method that calculates all candidate points is simple for implementation, large number of candidates are needed to obtain the accurate solution, bringing huge amount of calculation.

Therefore, in this section, we use the genetic algorithm (GA) to search for the optimal locations for hovering points. The genetic algorithm is a search algorithm based on the principles of biological evolution, incorporating genetic operations such as selection, crossover and mutation.

Selection

Roulette wheel selection is adopted for selection. The probability of the individual i being selected P_i is given as follows:

 doi:10.20944/preprints202504.0609.v1

$$P_i = \frac{f_i}{\sum_{j=1}^{N} f_j} \tag{12}$$

where f_i is the fitness function of i, which is defined as the number of UEs that can be covered from the location indicated by i. Parents of the next generation are selected according to the magnitude of the fitness function. Individuals with better fitness function are more likely to survive in the next generation.

Crossover

Blend crossover (BLX-α) [19] is adopted for crossover, with a crossover rate of 0.9. As shown in Figure 7, the coordinates of child individuals are generated in the area decided by the coordinates of parent individuals and parameter α. If we assume the coordinates of parent individuals are (x_1^p, y_1^p), (x_2^p, y_2^p), the coordinates of child individuals (x_1^c, y_1^c), (x_2^c, y_2^c) will be generated in the rectangular area created by point A, B, C, D as follows:

$$\mathrm{A} : (x_{\min} - \alpha dx, y_{\min} - \alpha dy) \tag{13}$$
$$\mathrm{B} : (x_{\min} - \alpha dx, y_{\max} + \alpha dy) \tag{14}$$
$$\mathrm{C} : (x_{\max} + \alpha dx, y_{\max} + \alpha dy) \tag{15}$$
$$\mathrm{D} : (x_{\max} + \alpha dx, y_{\min} - \alpha dy) \tag{16}$$

where dx, dy, $x_{\max}$, $x_{\min}$, $y_{\max}$, $y_{\min}$ are given as follows:

$$dx = |x_1^p - x_2^p| \tag{17}$$
$$dy = |y_1^p - y_2^p| \tag{18}$$
$$x_{\max} = \max(x_1^p, x_2^p) \tag{19}$$
$$x_{\min} = \min(x_1^p, x_2^p) \tag{20}$$
$$y_{\max} = \max(y_1^p, y_2^p) \tag{21}$$
$$y_{\min} = \min(y_1^p, y_2^p) \tag{22}$$

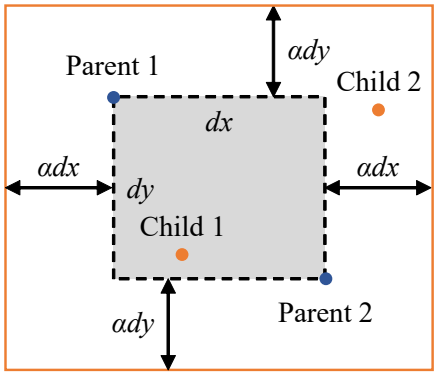

Figure 7. Sample of Blend Crossover

Mutation

Gaussian mutation is adopted for mutation, with a mutation rate of 0.005. Random individuals are generated according to the Gaussian distribution, preserving the diversity of the individuals.

 doi:10.20944/preprints202504.0609.v1

The process of searching for the optimal hovering point using GA is shown in Figure 8. From Figure 8, in contrast to the first generation, when the individuals are randomly distributed throughout the area, the individuals converge to where the UEs are densest after several generations. In this article, the maximum number of generations is set as 100. When it reaches the 100th generation, the individual with the highest fitness function will be selected as the hovering point. Then, the UEs which are already covered will be removed from the search by GA, and this process will be repeated until all remaining UEs are covered. While the result by GA is based on the maximum coverage radius of the UAV, i.e. the flight altitude is 150 m, it is necessary to apply the hill climbing algorithm to optimize the flight altitude.

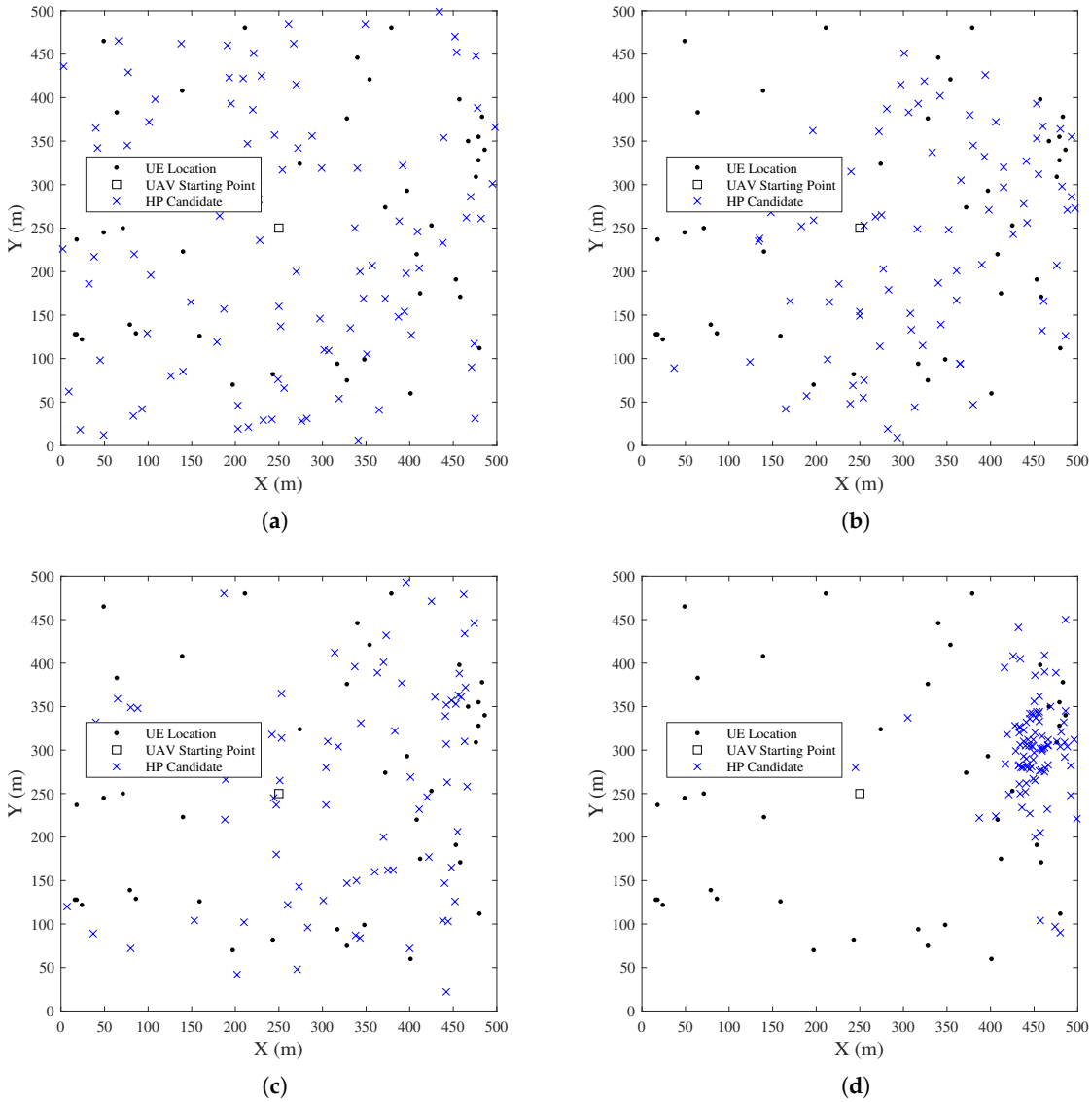

Figure 8. *Cont.*

Preprints.org (www.preprints.org) | NOT PEER-REVIEWED | Posted: 8 April 2025 doi:10.20944/preprints202504.0609.v1

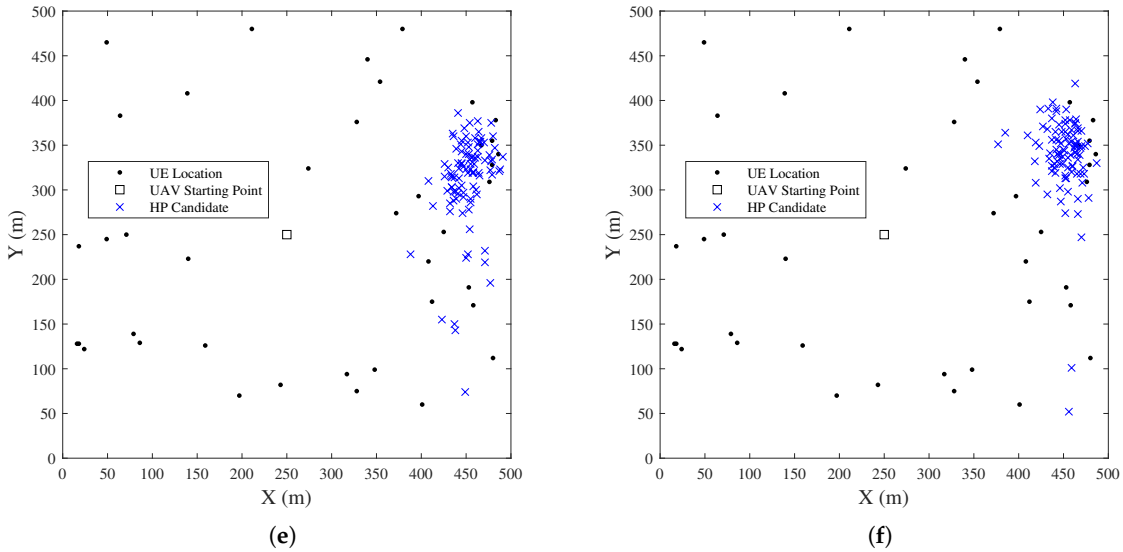

Figure 8. UE Clustering by K-Means: (**a**) 1st Generation (**b**) 3rd Generation (**c**) 5th Generation (**d**) 10th Generation (**e**) 15th Generation (**f**) 20th Generation.

4.3. Nearest Neighbor Search for Trajectory Decision

After the hovering points are decided, the trajectory which passes through all hovering points with the minimum flight time is needed to be decided. However, the TSP is known as an NP-hard problem, which needs huge amount of calculations to achieve the precise solution. Thus, for simplicity, we adopted the nearest neighbor search (NN), which is an approximate algorithm used in many applications.

As shown in Figure 9, according to the concepts of NN, the UAV always selects the nearest hovering point as the next destination.

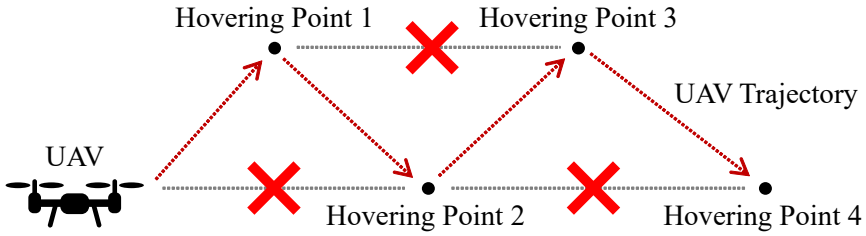

Figure 9. Sample of Nearest Neighbor Search

5. Simulation Results

5.1. Placement of Hovering Points

The placement of hovering points by sequenced k-means clustering is shown in Figure 10, where the blue and red dotted circles respectively indicate the coverage area before and after adopting the hill climbing algorithm. In this case, 12 is the smallest k to satisfy the flight altitude limitation. The cumulative distribution function (CDF) of the SNR before and after adopting the hill climbing algorithm is shown in Figure 11. From Figure 11, we can know that the hill climbing algorithm successfully optimized the UAV's flight altitude, achieving larger SNRs.

 doi:10.20944/preprints202504.0609.v1

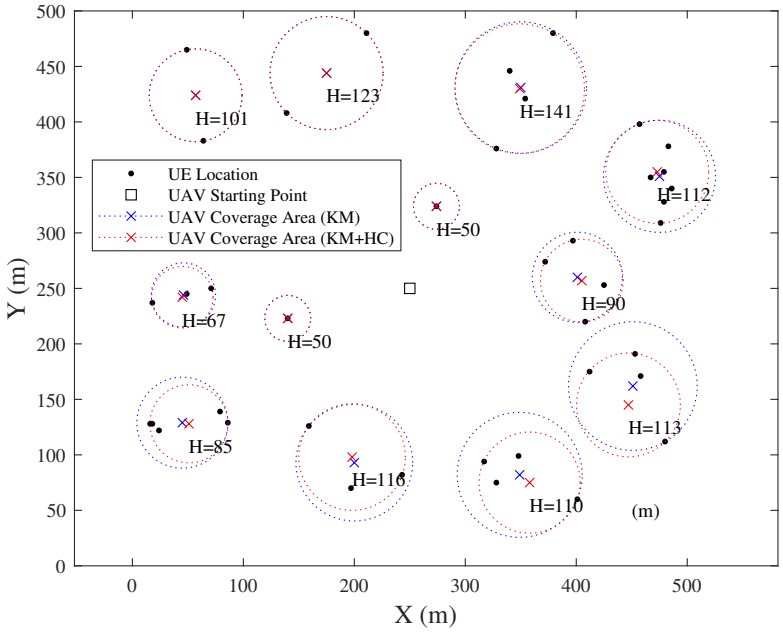

Figure 10. Hovering Points Placement by Sequenced K-Means Clustering

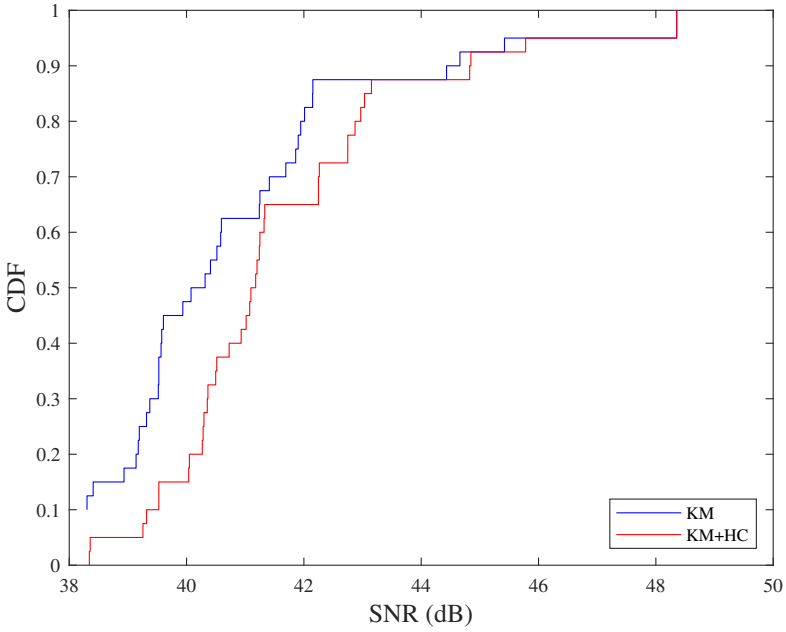

Figure 11. Comparison of SNR Before and After Using Hill Climbing Algorithm

Then, the placement of hovering points by GA is shown in Figure 12. The solution of the LSCP with the maximum flight height of 150 m, which is shown by the red dotted circles, is firstly obtained. And then, the hill climbing algorithm is adoted to optimize the UAV's flight altitude below 150 m, which is shown by the blue dotted circles.

 doi:10.20944/preprints202504.0609.v1

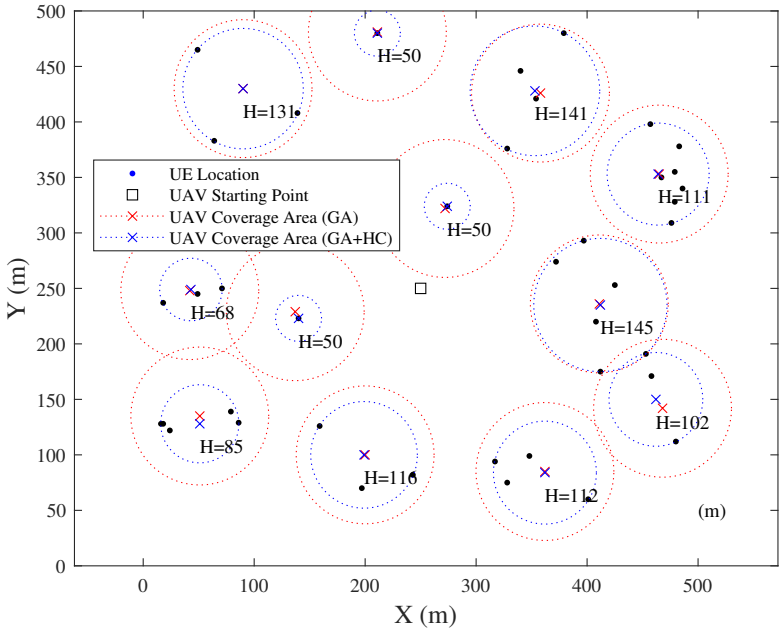

Figure 12. Hovering Points Placement by GA

The minimum number of hovering points obtained by sequenced k-means and GA is shown in Figure 13. From Figure 13, comparing to the traditional k-means clustering, the result by GA covers the same number of UEs with fewer hovering points, which indicates the improvement of the efficiency.

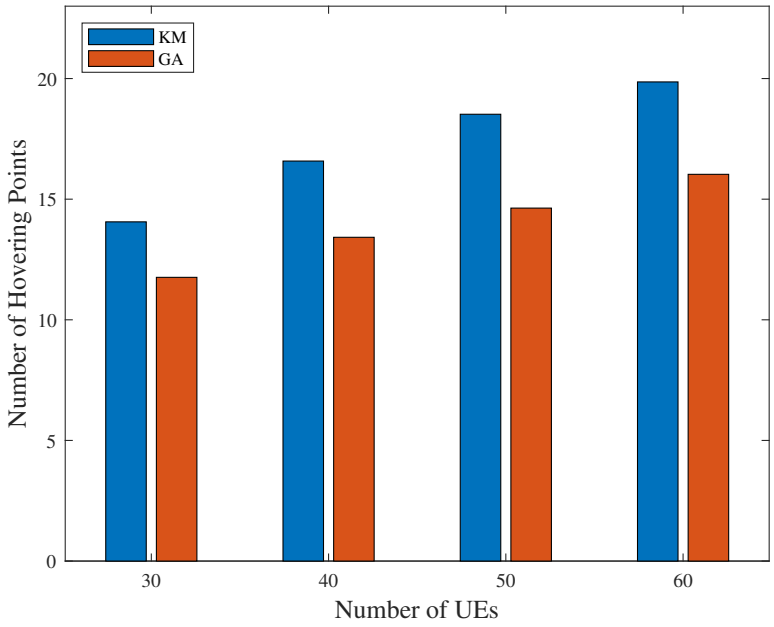

Figure 13. Minimum Number of Hovering Points by K-Means and GA

5.2. Trajectory Optimization

The UAV trajectories by previous method and proposed method are respectively shown in Figures 14 and 15. In previous method, the UAV's flight altitude is assumed as an constant, which is 100 m in Figure 14. The UAV needs to hover above each UE for data collection. This may increase the complexity of the trajectory, especially when the number of UEs increases. In contrast, the proposed method in this article i.e. 3-dimensional trajectory finishes the data collection with fewer hovering

 doi:10.20944/preprints202504.0609.v1

points by optimizing the flight altitude. The UAV covers and collects data from multiple UEs at the same location each time when hovering.

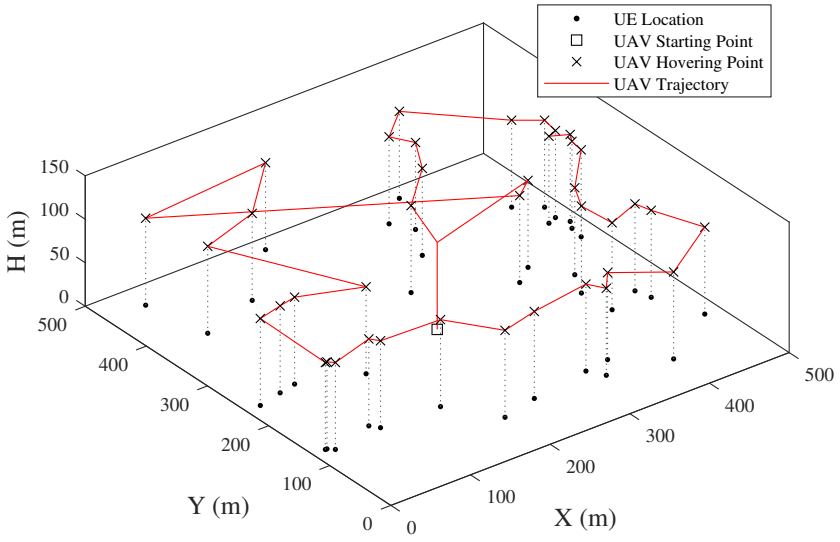

Figure 14. UAV Trajectory by Previous Method

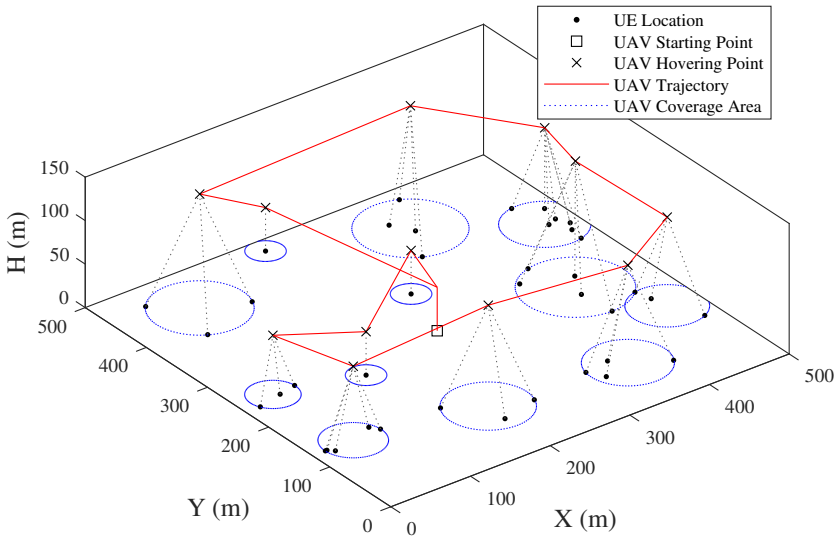

Figure 15. UAV Trajectory by Proposed Method

The results of the completion time with varying number of UEs are shown in Table 3 and Figure 16, where hovering time is the time for data transmission. From Table 3, it is clear that flight time occupies a large proportion in the mission completion time. The completion time, especially the flight time, is reduced by the proposed method, with the reduction rate of nearly 0.2. The hovering time slightly increases because of the increasement of UAV's flight altitude, which lowers the data rate.

 doi:10.20944/preprints202504.0609.v1

Table 3. Results of the Completion Time with Varying Number of UEs

Number of UEs	Total Time (s)		Flight Time (s)		Hovering Time (s)	
	Previous Method	Proposed Method	Previous Method	Proposed Method	Previous Method	Proposed Method
30	325.6855	282.3203	240.3592	195.8832	85.3263	86.4371
40	382.1829	327.8415	268.4145	210.7790	113.7684	117.0625
50	435.2349	371.6828	293.0245	224.9754	142.2105	146.7074
60	484.0537	410.4997	313.4011	233.1659	170.6526	177.3338
70	532.5094	446.7737	333.4147	239.3245	199.0947	207.4491
80	583.8943	484.3886	356.3576	246.9312	227.5368	237.4574

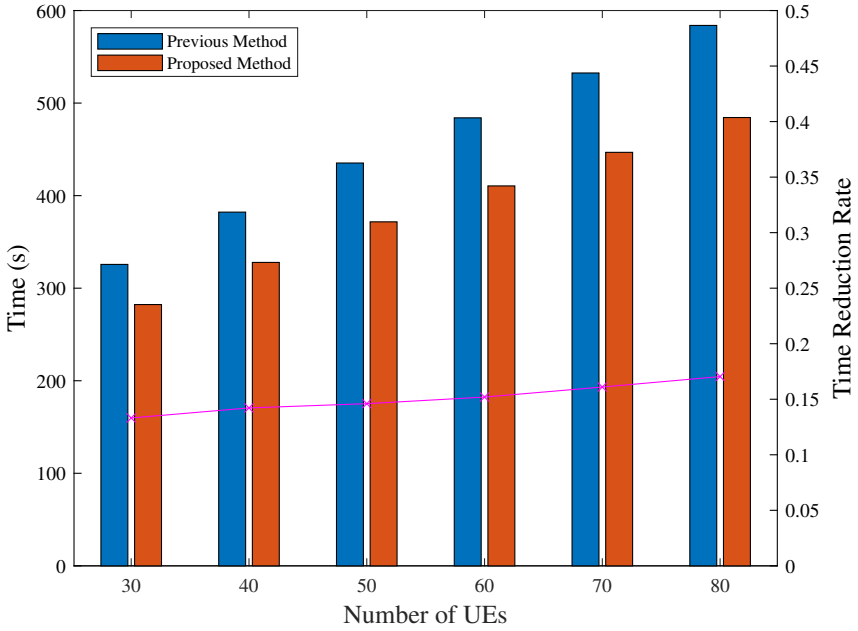

Figure 16. Completion Time with Varying Number of UEs

6. Conclusions

In this article, we considered the feasibility of UAV-based post-disaster data collection by proposing a 3-dimensional trajectory, which optimized the UAV's flight altitude. We transformed the problem to a LSCP solved by GA, and compared it with the traditional k-means clustering approach. From the simulation results, the proposed method showed better efficiency than the traditional k-means approach, covering all UEs with fewer number of hovering points. In addition, the effect of completion time reduction by the 3-dimensional trajectory proposed in this article is also confirmed, which indicates that the optimization of UAV's flight altitude is effective for completion time reduction.

However, this article focused on the optimization of UAV trajectory, which mainly contributes to the reduction of flight time. Although flight time occupies a large proportion in the mission completion time, the hovering time for data collection is also needed to be considered in future studies. Additionally, in real situations, environment conditions such as obstacles like buildings, weather such as wind, rain etc. also affect the flight of UAVs. For future issues of trajectory optimization, it is necessary to adapt advanced simulation models such as wind model, building model etc., and finally demonstration experiments are needed for further discussions.

Author Contributions: Conceptualization, R.Z. and G.K.T.; methodology, R.Z.; software, R.Z.; validation, R.Z.; formal analysis, R.Z.; investigation, R.Z.; data curation, R.Z.; writing—original draft preparation, R.Z.; writing—review and editing, G.K.T.; visualization, R.Z.; supervision, G.K.T. All authors have read and agreed to the published version of the manuscript.

 doi:10.20944/preprints202504.0609.v1

Funding: This research received no external funding.

Institutional Review Board Statement: Not applicable.

Informed Consent Statement: Not applicable..

Data Availability Statement: Data is contained within the article.

Conflicts of Interest: The authors declare no conflicts of interest.

References

1. Ministry of Internal Affairs and Communications. Communication Situation in the Great East Japan Earthquake (in Japanese). Available online: https://www.soumu.go.jp/johotsusintokei/whitepaper/ja/h23/pdf/n0010000.pdf (accessed on 25 February 2025).
2. National Institute of Information and Communications Technology. Disaster-Resilient Communication Networks: Introduction Guidelines (in Japanese). Available online: https://www.nict.go.jp/resil/pdf/guideline202006.pdf (accessed on 25 February 2025).
3. Yamamoto Town. Damage from the Great East Japan Earthquake and Tsunami (in Japanese). Available online: https://www.town.yamamoto.miyagi.jp/site/fukkou/324.html (accessed on 25 February 2025).
4. El Debeiki, M.; Al-Rubaye, S.; Perrusquía, A.; Conrad, C.; Flores-Campos, J.A. An Advanced Path Planning and UAV Relay System: Enhancing Connectivity in Rural Environments. *Future Internet* **2024**, *16*, 89.
5. Wang, W.; Wei, X.; Jia, Y.; Chen, M. UAV relay network deployment through the area with barriers. *Ad Hoc Networks* **2023**, *149*, 103222.
6. Chandran, I.; Vipin, K. Multi-UAV networks for disaster monitoring: Challenges and opportunities from a network perspective. *Drone Systems and Applications* **2024**, *12*, 1–28.
7. Zhang, Y.; Kuang, Z.; Feng, Y.; Hou, F. Task Offloading and Trajectory Optimization for Secure Communications in Dynamic User Multi-UAV MEC Systems. *IEEE Transactions on Mobile Computing* **2024**, *23*, 14427–14440.
8. Amrallah, A.; Mohamed, E.M.; Tran, G.K.; Sakaguchi, K. UAV Trajectory Optimization in a Post-Disaster Area Using Dual Energy-Aware Bandits. *Sensors* **2023**, *23*, 1402.
9. Zhang, T.; Lei, J.; Liu, Y.; Feng, C.; Nallanathan, A. Trajectory Optimization for UAV Emergency Communication With Limited User Equipment Energy: A Safe-DQN Approach. *IEEE Transactions on Green Communications and Networking* **2021**, *5*, 1236–1247.
10. Li, M.; Liu, X.; Wang, H. Completion Time Minimization Considering GNs' Energy for UAV-Assisted Data Collection. *IEEE Wireless Communications Letters* **2023**, *12*, 2128–2132.
11. Li, J.; Zhao, H.; Wang, H.; Gu, F.; Wei, J.; Yin, H.; Ren, B. Joint Optimization on Trajectory, Altitude, Velocity, and Link Scheduling for Minimum Mission Time in UAV-Aided Data Collection. *IEEE Internet of Things Journal* **2020**, *7*, 1464–1475.
12. Al-Hourani, A.; Kandeepan, S.; Lardner, S. Optimal LAP Altitude for Maximum Coverage. *IEEE Wireless Communications Letters* **2014**, *3*, 569–572.
13. Singh, A.; Redhu, S.; Hegde, R.M. UAV Altitude Optimization for Efficient Energy Harvesting in IoT Networks. *2022 National Conference on Communications (NCC)*, Mumbai, India, 2022, pp. 350–355.
14. Dai, X.; Duo, B.; Yuan, X.; Renzo, M.D. Energy-Efficient UAV Communications in the Presence of Wind: 3D Modeling and Trajectory Design. *IEEE Transactions on Wireless Communications* **2024**, *23*, 1840–1854.
15. Alzenad, M.; El-Keyi, A.; Yanikomeroglu, H. 3-D Placement of an Unmanned Aerial Vehicle Base Station for Maximum Coverage of Users With Different QoS Requirements. *IEEE Wireless Communications Letters* **2018**, *7*, 38–41.
16. Shannon, C.E. A Mathematical Theory of Communication. *The Bell System Technical Journal* **1948**, *27*, 379–423.
17. Ozasa, M.; Tran, G.K.; Sakaguchi, K. Research on the Placement Method of UAV Base Stations for Dynamic Users. *2021 IEEE VTS 17th Asia Pacific Wireless Communications Symposium (APWCS)*, Osaka, Japan, 2021, pp. 1–5
18. Toregas, C.; Swain, R.; ReVelle, C.; Bergman, L. The Location of Emergency Service Facilities. *Operations Research* **1971**, *19*, 1363–1373.
19. Eshelman, L.J.; David Schaffer, J. Real-Coded Genetic Algorithms and Interval-Schemata. *Foundations of Genetic Algorithms* **1993**, *2*, 187–202.

 doi:10.20944/preprints202504.0609.v1